Simulation of random mixed packing of different density particles*

Li Yuan-Yuan(李元元)[a], Xia Wei(夏 伟)[a], Zhou Zhao-Yao(周照耀)[a], He Ke-Jing(何克晶)[b]†, Zhong Wen-Zhen(钟文镇)[a], and Wu Yuan-Biao(吴苑标)[a]

[a] *School of Mechanical and Automotive Engineering, South China University of Technology, Guangzhou* 510641, *China*
[b] *School of Computer Science and Engineering, South China University of Technology, Guangzhou* 510641, *China*

(Received 22 February 2009; revised manuscript received 7 April 2009)

This paper presents the effects of density difference on the three-dimensional (3D) distribution of random mixed packing. The random mixed packing dynamics of particles of two different densities are simulated. The initial state is homogeneous, but the final packing state is inhomogeneous. The segregation phenomenon (inhomogeneous distribution) is also observed. In the final state, the top layers are composed of mostly light particles. The several layers beneath the top contain more heavy particles than light particles. At the bottom, they also contain more heavy particles than light particles. Furthermore, at both the top and the bottom, particle clustering is observed. The current study also analyses the cause of this inhomogeneity in detail. The main cause of this phenomenon is the velocity difference after collision of these two types of particles induced by the density difference. The present study reveals that even if particles were perfectly mixed, the packing process would lead to the final inhomogeneous mixture. It suggests that special treatment may be required to get the true homogeneous packing.

Keywords: mixed packing, different densities, granular particle, discrete element method simulation

PACC: 4610, 0320

1. Introduction

Packing is an essential step of many natural phenomena and industrial applications, such as the powder metallurgy (PM). In PM, the initial packing will affect the subsequent processes, and decide the quality of final products. The random packing of spherical particles has been studied for many years on account of its scientific, technological, and industrial importance. Starting from the 1970s, many scientists have used computer simulation methods to study the processes and properties, especially, the packing density, of random packing. For monosize spheres, most researches have gotten the packing density between 63% and 64%.[1] And for the mixed packing of particles of different sizes, three-dimensional (3D) packing densities above 75% have been reported.[2,3]

Although the mixed packing of particles of different sizes can be used to get a high packing density, mixed uses of different materials are more widely seen in industry. For instance, the powder of PM is almost alloy powder. Alloy powder is not only composed of particles with different radii, but is also composed of various kinds of metals with different densities. The different radii have a great effect on packing density which can decide the quality of the alloy. Little care is taken to study the inhomogeneity caused by different densities, which also has a great impact on the structure and the mechanical property of alloy parts. Although the mixed packing of different density particles is important for getting high quality PM products, it has been less studied previously. Most of the studies assume that the structure of particles is homogeneous, but actually, it is inhomogeneous. There has been little research about particles with different density and distribution of particles in gravity. Fiske *et al.*[4] experimentally studied the segregation phenomena of spherical and nonspherical particles due to size difference. Recently, Shi *et al.*[5] experimentally studied the segregation in vertically vibrated binary granular mixtures with identical sizes but different densities and Yang[6] studied the same phenomena by simulation. The time evolution of pattern formations showed that the heavy particles first move toward the centre of the

*Project supported by the State Key Development Program for Basic Research of China (973 Program) (Grant No. 2007CB616905), the National High Technology Research and Development Program of China (863 Program) (Grant No. 2007AA03Z112), the National Natural Science Foundation of China (Grant No. 10805019), and the Natural Science Foundation of Guangdong Province of China (Grant No. 8451064101000083).

†Corresponding author. E-mail: kejinghe@ieee.org

© 2010 Chinese Physical Society and IOP Publishing Ltd

bed and then concentrate near the centres of the two convection cells of the vibrated system. Their study mainly focuses on the effects of different density particles on the vibrated mixing (the mixing stage). What they studied is the dynamics of one layer spheres in a flat tank, and the segregation phenomenon is observed.

The main objective of the present research is to study the 3D distribution of random mixed packing (the packing stage) of the binary mixture with equal sizes but different densities. Perfect mixed particles are assumed and poured into a real 3D container to study the density effect on the final packing properties. The segregation phenomenon (inhomogeneous distribution) is also observed. More light particles are found at the top layers, and more heavy particles are found at the bottom. The influences of this density effect on the final product quality are also discussed carefully. This paper is organized as follows. Following the introduction in Section 1, Section 2 explains the simulation models and methods. Section 3 describes the result and process of random mixed packing. The initial distribution, the final state, the speed histograms of key steps, and the cause of final inhomogeneity are analysed in detail. Finally, some conclusions and discussions are made in Section 4.

2. Simulation model and method

The discrete element method (DEM)[7] has proven itself as a valuable tool to investigate the packing process. As the prior researches had adopted DEM to study the dynamics and properties of gravity-deposited systems of spherical particles,[3,8] DEM was used to simulate the particle dynamics in this study. The governing equations of motion for particle i are

$$m_i \frac{\mathrm{d}\boldsymbol{v}_i}{\mathrm{d}t} = \sum_j (\boldsymbol{F}_{\mathrm{cn},ij} + \boldsymbol{F}_{\mathrm{dn},ij} + \boldsymbol{F}_{\mathrm{ct},ij}) + mg, \quad (1)$$

$$I_i \frac{\mathrm{d}\omega_i}{\mathrm{d}t} = \sum_j (\boldsymbol{R}_i \times \boldsymbol{F}_{\mathrm{ct},ij}), \quad (2)$$

where m_i, $\boldsymbol{v}_i$, I_i, and ω_i are the mass, translational velocity, moment of inertia, and angular velocity of particle i, respectively. $\boldsymbol{F}_{\mathrm{cn},ij}$, $\boldsymbol{F}_{\mathrm{dn},ij}$ and $\boldsymbol{F}_{\mathrm{ct},ij}$ are the contact force in normal direction, the damping force in normal direction and the contact force in tangential direction, respectively, of particle i due to particle j. $\boldsymbol{R}_i$ is a vector running from the centre of particle to the contact point with its magnitude equal to particle radius R_i. A simple linear elastic-damping model is adopted.

$$\boldsymbol{F}_{\mathrm{cn},ij} = k_{\mathrm{n}} \xi_{\mathrm{n}} \hat{\boldsymbol{n}}_{ij}, \quad (3)$$

where k_{n} is the normal elastic constant, ξ_{n} is the displacement in normal direction, and $\hat{\boldsymbol{n}}_{ij}$ is the unit vector point from the centre of particle j to the centre of particle i.

The damping in normal direction $\boldsymbol{F}_{\mathrm{dn},ij}$ is

$$\boldsymbol{F}_{\mathrm{dn},ij} = -\gamma_{\mathrm{n}} |\boldsymbol{F}_{\mathrm{cn},ij}| \mathrm{sign}(\dot{\xi}_{\mathrm{n}}), \quad (4)$$

where γ_{n} is the damping constant in the normal direction. The hysteretic damping model applied here is similar to the model proposed by Walton and Braun.[9]

The elastic model in tangential direction is adopted from Cundall and Strack,[7] in which a tangential "virtual" spring is put at the contact point when two particles start to touch each other

$$\boldsymbol{F}_{\mathrm{cs},ij} = -\min\left(|k_{\mathrm{s}}\xi_{\mathrm{s}}|, |\mu(\boldsymbol{F}_{\mathrm{cn},ij} + \boldsymbol{F}_{\mathrm{dn},ij})|\right) \times \mathrm{sign}(\xi_{\mathrm{s}}), \quad (5)$$

where k_{s} is the tangential elastic constant, and ξ_{s} is the total shear displacement of the tangential spring that took place since the time t_0 when the contact was first established, i.e.

$$\xi_{\mathrm{s}} = \int_{t_0}^{t_1} \boldsymbol{v}_{\mathrm{s}}(t)\mathrm{d}t. \quad (6)$$

Since the complexity of direct computing of all interparticle forces is $O(N^2)$, the $O(N)$ multigrid contact detection method[3] is adopted to get these contacted particle pairs before conducting the actual calculation.

The simulation is composed of two stages, namely, the initial stage and the settling stage. To avoid the instability caused by the initial overlaps of random placed particles, a "growing process" is introduced in the initial stage. At the beginning of the initial stage, particles are initialized with radii equal to zero and are placed within a rectangular box randomly. At the initial stage, the particles are growing to their target radii gradually, and the contacts are detected and processed. Then the simulation switches to the settling stage. At the settling stage, gravity is switched on, particles move according to gravity and inter-particle forces. The system energy will be dissipated by damping and particles will reach their stable position eventually. For a more detailed description of the system, see He *et al.*[3,10]

In this application, the simulation time step Δt is 50 μs, the initial stage lasts 4000 steps (0.2 s), and the whole simulation lasts 60000 steps (3 s). The

system includes 6000 particles (3000 light ones and 3000 heavy ones). The size of the rectangular box is 1 m × 1 m ×1 m. Periodic boundary conditions are applied to four vertical walls. No top boundary condition is applied and the bottom wall has the same physical property as particles. Other simulation parameters are listed in Table 1, where the densities of heavy particles and light particles are represented by $\rho_{\rm H}$ and $\rho_{\rm L}$ respectively. The damping constant in the normal direction ($\gamma_{\rm n}$) is set according to Zhong *et al.*[11]

Table 1. Parameters for the simulation of particle packing.

parameter	value	parameter	value
$k_{\rm n}$	10^7 N/m	$k_{\rm s}$	10^7 N/m
μ	0	$\gamma_{\rm n}$	0.7
$N_{\rm H}$	3000	$N_{\rm L}$	3000
$\rho_{\rm H}$	7800 kg/m^3	$\rho_{\rm L}$	1200 kg/m^3
R	0.02 m	g	9.8 m/s^2

3. Results and discussion

3.1. Inhomogeneous distribution of final state

In many industrial processes, engineers meet a homogeneous mixture of different particles (e.g. different sizes, different densities). To get this perfect state, particles are usually mixed first by using a shaker or mixer, and then poured into the mold. To examine whether this approach can get the real homogeneous packing, homogenized mixture is assumed and its packing process is simulated. The simulation starts with random generated particles, as illustrated in Fig. 1. Two types of particles with the same size but different densities are included into the system.

The whole simulation lasts 60000 steps (3 s), and the final stable state is illustrated in Fig. 2. Though at the beginning, heavy particles and light particles are homogeneously mixed, the segregation phenomenon is obvious in the final state. Yang[6] studied the particle distribution of binary granular mixing and also found that the density in the upper region for light particles is larger than that of heavy particles during the mixing process. Since all other parameters of the two types of particles are the same except the densities, the cause of the segregation can only be the density difference. The experiments of Shi *et al.*[5] about the effects of different density particles on the vibrated mixing also suggest that the density ratio is the most important factor for the final segregation.

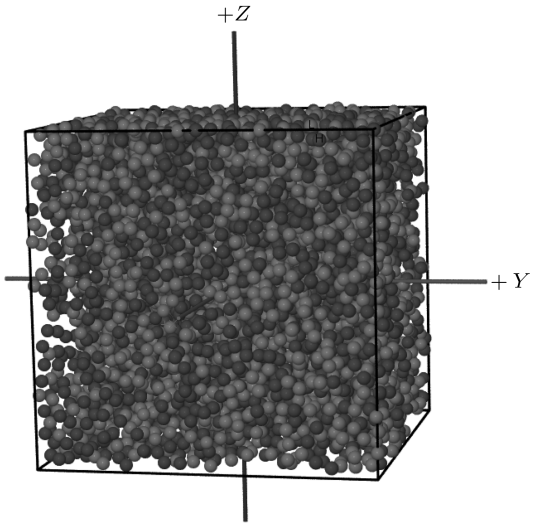


Fig. 1. Particle distribution of initial state. Light particles are colored grey in the color mode (light grey in the grey mode), and one of them is marked "L". Heavy particles are colored blue in the color mode (dark grey in the grey mode), and one of them is marked "H". This color scheme will be used throughout the whole paper.

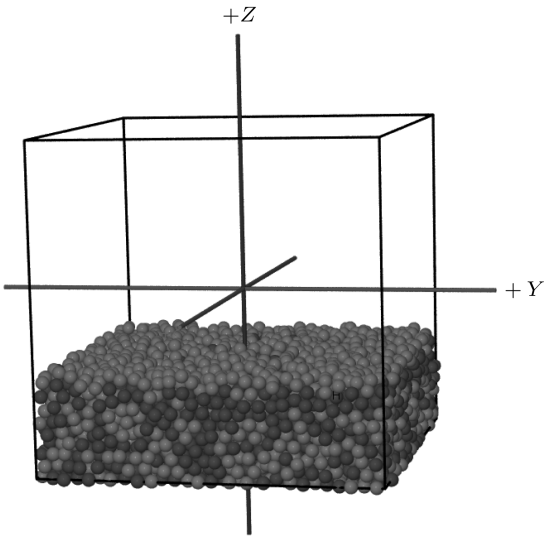


Fig. 2. Particle distribution of the final state.

Figure 3 presents the cross sectional proportion of light particles ($P_{\rm L}$) at different vertical coordinates of the final state. The Z coordinate of the bottom is defined as zero. The percentage proportion is defined as

$$P_{\rm L}(Z) = \frac{\sum\limits_{i|\rho_i=\rho_{\rm L}} \pi \max\left(0, R_i^2 - (Z - Z_i)^2\right)}{\sum\limits_{i} \pi \max\left(0, R_i^2 - (Z - Z_i)^2\right)}. \quad (7)$$

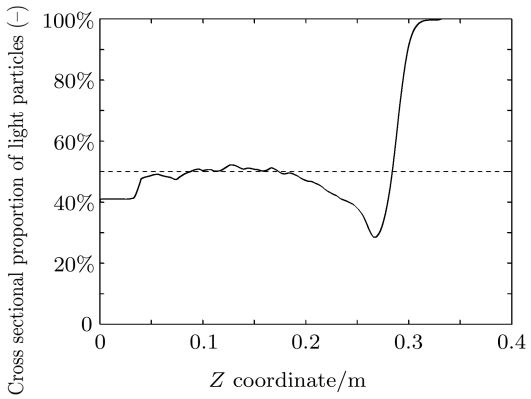


Fig. 3. The cross sectional proportion of light particles at different $+Z$ coordinates of the final state.

Since there are only two types of particles in the system, the proportion of heavy particles equals 100% minus the proportion of light particles ($P_{\mathrm{H}} = 1 - P_{\mathrm{L}}$). As shown in Fig. 3, the top layers are mostly composed of light particles. We can also observe this from Fig. 2. The several layers beneath the top contain more heavy particles than light particles. This segregation is caused by the collision of heavy particles and light particles in the top layers, which will be analysed in detail later.

An interesting observation is the inhomogeneous distribution of light and heavy particles at the bottom. There are less light particles than heavy particles from the bottom to height (Z) equal to about 0.04 m. It is worth while noting in the present study, the radii of particles are 0.02 m (half of 0.04 m), which imply that the bottom layer contains about 40% light particles and 60% heavy particles. This is because the light particles are more energetic than heavy particles after their interparticle collisions and colliding to the bottom wall. So, light particles tend to rise higher than heavy particles, resulting in the decrease of light particle proportion at the bottom. Another contributing factor is the loose density of the initial state. The interparticle spaces allow the free movement of bottom particles to some extent. More heavy particles at the bottom also conform to the theorem of minimum potential energy. To our knowledge, although the bottom inhomogeneity will also affect the final product quality, no one has reported it before.

Figures 4 and 5 illustrate the top view and bottom view of the final state respectively. Clustering is obvious in both views. It means that even if different density particles are perfectly mixed and homogenized before packing, the packing process may also cause clustering and inhomogeneous final distribution.

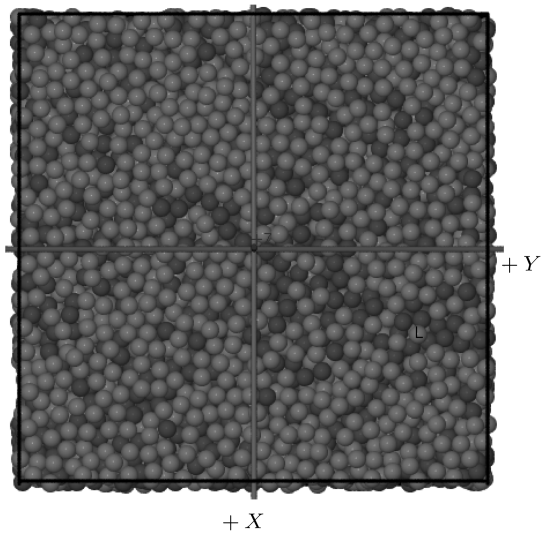


Fig. 4. The top view of the final state.

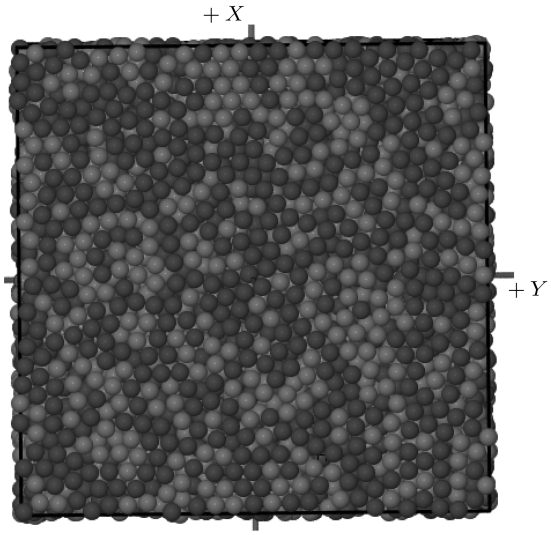


Fig. 5. The bottom view of the final state.

3.2. The cause of final inhomogeneity

To investigate the cause of the inhomogeneity at the top layers, the key steps of the packing process are analysed in detail. Figure 6 illustrates the particle distribution at simulation step 10000 ($t = 0.5$ s). It is before the collisions of top layer particles. The distribution of particles is still homogeneous.

Figure 7 illustrates the speed histogram of light particles and heavy particles at simulation step 10000 ($t = 0.5$ s). There are around 1250 heavy particles and 1400 light particles whose speed exceeds 1 m/s. This is because most particles have not collided heavily yet, the gravitational potential energy is converted to the

kinetic energy during the free fall process, resulting in many high speed particles.

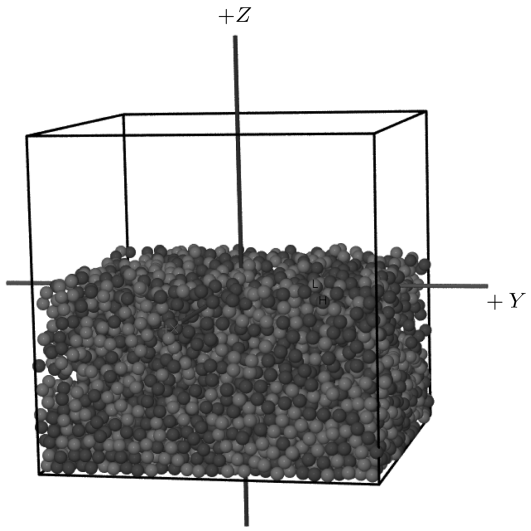


Fig. 6. Particle distribution at simulation step 10000 ($t = 0.5$ s, before the collisions of top layer particles).

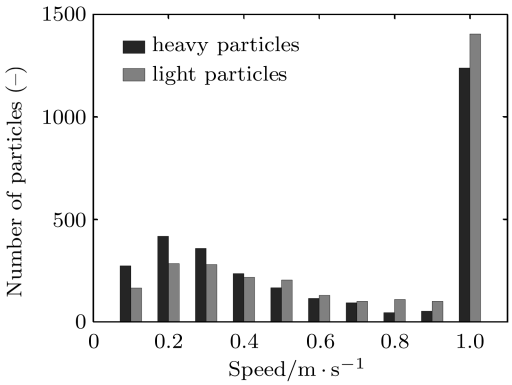


Fig. 7. Speed histogram of particles at simulation step 10000 ($t = 0.5$ s).

Figure 8 illustrates the histogram of Z coordinates of those particles whose speed is greater than 1 m/s. Since the collisions at the bottom dissipated a lot of energy, there are only a few high speed particles there. In the two to three layers above the bottom (Z = 0.1 m–0.2 m), there are much more high speed light particles than heavy particles. It confirms that light particles can achieve higher speed than heavy particles from the interparticle collisions. From $Z = 0.2$ m to $Z = 0.5$ m, the histogram almost follows a uniform distribution, which means that particles are in the free-falling stage and there is little collision between them.

Figure 9 illustrates the particle distribution at simulation step 12000 ($t = 0.6$ s) when the collisions of top particles were just happened. Figure 10 illustrates the speed histogram of all particles at step 12000. The speed of most particles is very small, but there are around 150 light particles whose speed is greater than 1 m/s (marked with an ellipse).

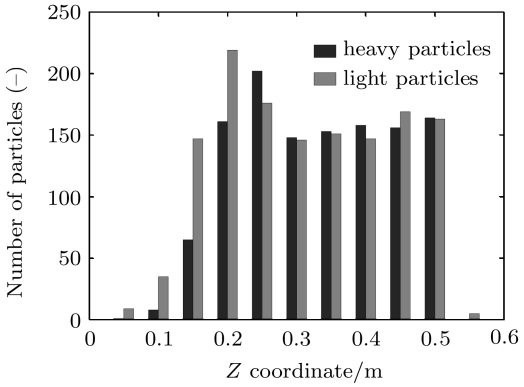


Fig. 8. Histogram of Z coordinates of particles whose speed is greater than 1 m/s (step 10000, $t = 0.5$ s).

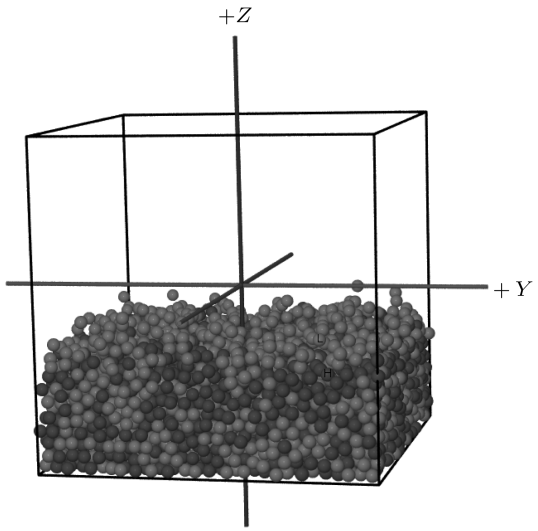


Fig. 9. Particle distribution at simulation step 12000 ($t = 0.6$ s, after the collisions of top layer particles).

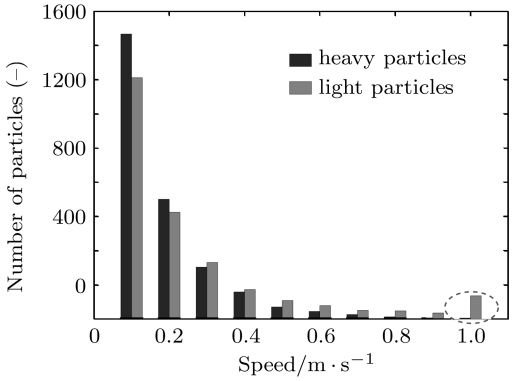


Fig. 10. Speed histogram of particles at simulation step 12000 ($t = 0.6$ s).

Figure 11 illustrates the histogram of Z coordinates of high speed particles at simulation step 12000

($t = 0.6$ s). After the collision of top particles, there are much more high speed light particles than high speed heavy particles.

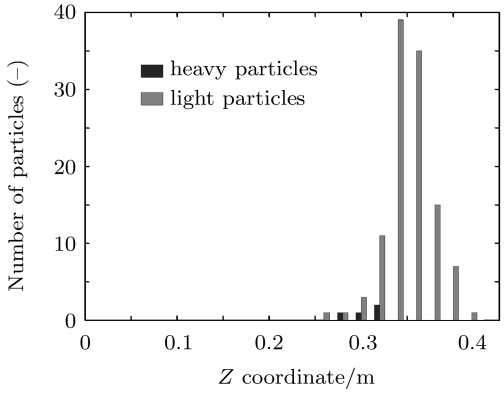


Fig. 11. Histogram of Z coordinates of particles whose speed is greater than 1 m/s (step 12000, $t = 0.6$ s).

According to the impulse-momentum theorem described by

$$P_{\mathrm{t}} = m\Delta v, \tag{8}$$

where P_{t} is the impulse, m is the mass and Δv is the change of velocity, light particles are easier to get higher speed in the collision with heavy particles. After the collision, light particles are likely to move farther than heavy particles. However, actually, most light particles cannot move too long. The length of the mean free path is very short, and they will collide with some other particles quickly and the kinetic energy is also quickly dissipated. Only the light particles located at the top have chances to get high speed toward the $+Z$ direction and escape the successive collisions, resulting in the final state where the top layer is almost occupied by light particles.

4. Conclusions

This paper simulated the random mixed packing process of particles of two different densities. The initial state is homogeneous, but the final packing state is inhomogeneous. In the final state, the top layers are composed of most light particles. The several layers beneath the top contain more heavy particles than light particles. At the bottom, they also contain more heavy particles than light particles. Furthermore, at both the top and the bottom, particle clustering is observed. The current study also analysed the cause of this inhomogeneity in detail. The main cause of this phenomenon is the different densities of these two types of particles. At the top, light particles achieve a higher speed than heavy particles after the interparticle collisions. Consequently, they can move higher and finally occupy most of the top layer space. At the bottom, high speed light particles also have some spaces to move upward, resulting in the uneven distribution of particles.

The current study reveals that even if particles were perfectly mixed, the packing process would lead to the final inhomogeneous mixture. This inhomogeneous distribution will influence the final product quality. For instance, in the power metallurgy, uneven distributed particles will lead to the inhomogeneous density distribution (low quality) of the final product. It suggests that special treatment may be required to get the true homogeneous packing.

References

[1] Scott G D and Kilgour D M 1969 *J. Phys.* D: *Appl. Phys.* **2** 863
[2] Stroeven P and Stroeven M 1999 *Cement and Concrete Research* **29** 1201
[3] He K J, Dong S B and Zhou Z Y 2007 *Phys. Rev.* E **75** 036710
[4] Fiske T J, Railkar S B and Kalyon D M 1994 *Powder Technology* **81** 57
[5] Shi Q, Sun G, Hou M and Lu K 2007 *Phys. Rev.* E **75** 061302
[6] Yang S C 2006 *Powder Technology* **164** 65
[7] Cundall P A and Strack O D L 1979 *Géotechnique* **29** 47
[8] Zhang Z P, Liu L F, Yuan Y D and Yu A B 2001 *Powder Technology* **116** 23
[9] Walton O R and Braun R L 1986 *Journal of Rheology* **30** 949
[10] Zhong W Z, He K J, Zhou Z Y, Xia W and Li Y Y 2009 *Acta Phys. Sin.* **58** S21 (in Chinese)
[11] Zhong W Z, He K J, Zhou Z Y, Xia W and Li Y Y 2009 *Acta Phys. Sin.* **58** 5155 (in Chinese)